Turkish Journal of Electrical Engineering & Computer Sciences

http://journals.tubitak.gov.tr/elektrik/

Research Article

Turk J Elec Eng & Comp Sci
(2018) 26: 1812 – 1819

doi:10.3906/elk-1706-309

Lorenz-like system design using cellular neural networks

Enis GÜNAY[1], **Kenan ALTUN**[2,*]
[1]Department of Electrical and Electronics Engineering, Faculty of Engineering, Erciyes University, Kayseri, Turkey
[2]Sivas Vocational College, Cumhuriyet University, Sivas, Turkey

Received: 26.06.2017 • **Accepted/Published Online:** 15.05.2018 • **Final Version:** 27.07.2018

Abstract: In this study, a Lorenz-like system based on cellular neural networks (CNNs) is proposed. Complex butterfly chaotic attractors of Lorenz-like systems are constructed using a three-cell CNN. The proposed system makes the CNN imitate quadratic system dynamics without altering its output nonlinearity. Experimental and numerical analysis results are presented in order to verify the convenience of the system.

Key words: State-controlled cellular neural networks, Lorenz system, multivariable nonlinearity, complex dynamics, Lorenz-like systems

1. Introduction

In the past decade, understanding and analyzing chaos has evolved into utilizing chaos in the field of applied chaos theory. Many studies have focused on the design of nonlinear circuits to analyze and generate chaos. These studies have had a significant role in providing a basis for further development of nonlinear circuits. The flap of a butterfly's wings in Brazil did not set off a breeze in Texas, but caused a tornado in the field of nonlinear systems and chaos. Because of its unique lemniscate shape, the Lorenz system has been the origin of many chaos-based applications [1–3]. In addition, several other systems with similar behavior, such as Chen's system, Liu's system, and Rikitake's system [3–5], have also been studied. While these systems can be called Lorenz-like, they are also members of a quadratic system family in R^3 depending on the parameters.

On the other hand, cellular neural networks (CNNs) have attracted considerable attention and there have been many theoretical and experimental studies of CNNs in the literature since their introduction [6–8]. Various CNN-based chaotic and nonlinear circuits have been presented in the literature, after the introduction of the state controlled-CNN (SC-CNN) [9]. The generalized dimensionless nonlinear state equations of the SC-CNN are given as follows:

$$\begin{aligned} \dot{x}_j &= -x_j + a_j y_j + G_0 + G_s + i_j \\ y_j &= \tfrac{1}{2}\left[|x_j+1| - |x_j-1|\right] \end{aligned}, \qquad (1)$$

where j is the index of the cell, x_j is the state variable, y_j is the output of the cell, a_j is a constant, i_j is the threshold, G_0 is the output, and G_s is the state variables of the connected cells. SC-CNN-based systems not only offer RC-based, multiplier-free, and ready-to-integrate process designs, but also offer a flexible system that can be easily converted to different chaos generators merely by adjusting the connection weights.

*Correspondence: kaltun@cumhuriyet.edu.tr

The primary disadvantage of the SC-CNN-based systems is the representation of system nonlinearity using only one state variable [10–12]. The output function of the SC-CNN expressed in Eq. (1) is a one-dimensional piecewise-linear (PWL) function. If the nonlinearity of a system is obtained by the products of state variables, then a one-dimensional PWL output function is insufficient to represent its behavior. To deal with this insufficiency, SC-CNN's PWL output function was replaced with PWL approximations where the nonlinearity is obtained with the squares of state variables. In the literature, the dynamics of the original Rössler system was mapped with an extended SC-CNN using a PWL that can approximate the nonlinearities as squares of state variables [13,14]. Such an extension causes an increase in the circuitry and complexity of the SC-CNN.

In the present study, to overcome this insufficiency, the nonlinearity of the Lorenz-like system is modeled via an SC-CNN architecture by switching the sign of the states depending on the PWL output function of the SC-CNN. The bipolar voltage-controlled switching parameter has the ability to reproduce quadratic system dynamics without changing the original PWL output of the SC-CNN.

In Section 2, a SC-CNN–based Lorenz-like system is introduced after a brief explanation of the original Lorenz system, and the numerical analysis results are presented. In Section 3, the experimental results are presented. Finally, Section 4 is the conclusion.

2. SC-CNN–based Lorenz-like systems

The Lorenz system, which was introduced in 1963 [15], consists of three nonlinear differential equations with two product-type nonlinearities (xz and xy), as shown in Eq. (2).

$$\begin{aligned} \dot{x} &= a(y-x) \\ \dot{y} &= (b-z)x - y \\ \dot{z} &= xy - cz \end{aligned} \tag{2}$$

Here a, b, and c represent the constants. The product-type nonlinearity is responsible for the generation of chaos. Generation of multivariable nonlinearity in conventional SC-CNN always seems to be a problem because of the PWL output function given in Eq. (1). To deal with this problem, Eq. (1) can be rearranged as follows:

$$\begin{aligned} \dot{x}_j &= -x_j + a_j y_j + G_0 + G_s + G_n + i_j \\ y_j &= \tfrac{1}{2}\left[|x_j+1| - |x_j-1|\right] \end{aligned}, \tag{3}$$

where j represents the cell index. The switched SC-CNN system presented in Eq. (3), perfectly fits with the conventional SC-CNN except for the presence of G_n state variables. The quadratic functions of the state variables can be simulated using G_n, which is the bipolar voltage-controlled switching parameter. Three CNN cells derived from Eq. (3) can be written as follows:

$$\dot{x}_1 = -x_1 + \sum_{k=1}^{3} a_{1k} y_k + \sum_{k=1}^{3} s_{1k} x_k + \sum_{k=1}^{3} n_{1k} x_k + i_1$$

$$\dot{x}_2 = -x_2 + \sum_{k=1}^{3} a_{2k} y_k + \sum_{k=1}^{3} s_{2k} x_k + \sum_{k=1}^{3} n_{2k} x_k + i_2 \tag{4}$$

$$\dot{x}_3 = -x_3 + \sum_{k=1}^{3} a_{3k} y_k + \sum_{k=1}^{3} s_{3k} x_k + \sum_{k=1}^{3} n_{3k} x_k + i_3,$$

where k represents the cell index. Here $x$is the state variable, y is the cell output, a is the feedback from the output of neighbor cells, and s is the feedback from the states of the neighbor cells with threshold i. Additionally, n is a bipolar voltage-controlled switching parameter that simulates the possible quadratic variations of the state variables. A Lorenz-like system can be generated by choosing the parameters as follows:

$$s_{13} = s_{23} = s_{31} = s_{32} = 0, a_{11} = a_{12} = a_{13} = a_{21} = a_{22} = a_{23} = a_{31} = a_{32} = a_{33} = 0,$$

$$s_{11} = s_{12} = s_{21} = 1, s_{22} = 0.5, s_{33} = 0.75, i_3 = 0.2,$$

$$n_{11} = n_{12} = n_{13} = n_{21} = n_{22} = n_{32} = n_{33} = 0,$$

$$n_{23} = sgn(y_1), n_{31} = sgn(x_1 - i_3),$$

$$y_1 = \frac{1}{2}\left[|x_1 + 1| - |x_1 - 1|\right]$$

$$\dot{x}_1 = -x_1 + s_{11} x_1 + s_{12} x_2$$

$$\dot{x}_2 = -x_2 + s_{21} x_1 - s_{22} x_2 + n_{23} x_3 \tag{5}$$

$$\dot{x}_3 = -x_3 + s_{33} x_3 + n_{31}(x_1 + i_3)$$

Using$n$ coefficients as switches with zero thresholds, $\dot{x}_2$ and $\dot{x}_3$ operate as dual systems with two complementary modes of operation.

$$n_{23} = \begin{cases} -1; \ y_1 \geq 0 \\ +1; \ y_1 < 0 \end{cases}$$

$$n_{31} = \begin{cases} +1; (x_1 - i_3) \geq 0 \\ -1; \ (x_1 - i_3) < 0 \end{cases} \tag{6}$$

$$\left.\begin{array}{l} \dot{x}_2 - = -x_2 + s_{21} x_1 - s_{22} x_2 - x_3, \\ \dot{x}_3 + = -x_3 + s_{33} x_3 + (x_1 + i_3), \end{array}\right\} \qquad y_1 \geq 0 \, and \, (x_1 - i_3) \geq 0$$

$$\left.\begin{array}{l} \dot{x}_2 + = -x_2 + s_{21} x_1 - s_{22} x_2 + x_3, \\ \dot{x}_3 - = -x_3 + s_{33} x_3 - (x_1 + i_3), \end{array}\right\} \qquad y_1 < 0 \, and \, (x_1 - i_3) < 0$$

3. Numerical analysis

For the initial conditions $x_1(0.1)$, $x_2(0.1)$, $x_3(0)$, the equilibrium points of Eq. (5) exist in two subspaces defined as

$$D_+ = (x_1, x_2, x_3) \left| y_1 and \, (x_1 - i_1) \geq 0 : P^+ = (-k_1, -k_2, -k_3), \right.$$

$$D_- = (x_1, x_2, x_3) \left| y_1 and \, (x_1 - i_1) < 0 : P^- = (k_1 k_2 k_3), \right. \tag{7}$$

for $n_{23} = \pm 1$ and $n_{31} = \pm 1$:

$$k_1 = \frac{-(i_3 s_{12})}{(s_{12} - s_{11} + s_{22} - s_{33} - s_{11}s_{22} - s_{12}s_{21} + s_{11}s_{33} - s_{22}s_{33} + s_{11}s_{22}s_{33} + s_{12}s_{21}s_{33} + 1)},$$

$$k_2 = \frac{-(i_3 - i_1 s_{11})}{(s_{12} - s_{11} + s_{22} - s_{33} - s_{11}s_{22} - s_{12}s_{21} + s_{11}s_{33} - s_{22}s_{33} + s_{11}s_{22}s_{33} + s_{12}s_{21}s_{33} + 1)},$$

$$k_3 = \frac{-(-i_3 + i_3 s_{11} - i_3 s_{22} + i_3 s_{11}s_{22} + i_3 s_{12}s_{21})}{(s_{12} - s_{11} + s_{22} - s_{33} - s_{11}s_{22} - s_{12}s_{21} + s_{11}s_{33} - s_{22}s_{33} + s_{11}s_{22}s_{33} + s_{12}s_{21}s_{33} + 1)},$$

The equilibrium points P^+ and P^- can be obtained from the *Jacobian matrices* as

$$J_+ = \begin{vmatrix} (s_{11} - 1) & s_{12} & 0 \\ s_{21} & (-s_{22} - 1) & -1 \\ 1 & 0 & (s_{33} - 1) \end{vmatrix}$$

$$J_- = \begin{vmatrix} (s_{11} - 1) & s_{12} & 0 \\ s_{21} & (-s_{22} - 1) & 1 \\ -1 & 0 & (s_{33} - 1) \end{vmatrix} \tag{8}$$

Eigenvalues for the equilibrium points (–4/15, 0, –4/15) ? D_+ and (–4/15, 0, 4/15) ? D_-, which are calculated from the matrix J_+ and the matrix J_- respectively, are determined as $\lambda_1 = –1.5941$, $\lambda_{2,3} = 0.4220 \pm i0.5407$. λ_1 is a negative real number, and $\lambda_{2,3}$ are complex conjugate eigenvalues with positive real parts. Thus the proposed switched SC-CNN system is unstable and the equilibrium point P is a saddle-focus. A period-doubling scenario is shown in Table 1.

Table 1. Bifurcation parameter values.

Bifurcation	s_{22}
period-1 period-2	0.5–0.5012
period-2 period-4	0.5012–0.5058
period-4 period-8	0.5058–0.5068
period-8 period-16	0.5068–0.507
period-16 chaos	0.507–...

From Table 1 it can be seen that the attractor undergoes a period-doubling bifurcation, which converts it from a period-1 to a period-2 attractor, when the parameter s_{22} exceeds a critical value around 0.5012. As we continue to increase s_{22} gradually, the attractor undergoes period-doubling bifurcation at $s_{22} = 0.5058$, and period-2 attractor becomes period-4. Period-8 and period-16 attractors are overcome as s_{22} reaches 0.5068 and 0.507, respectively. Shortly after period-16, the various curves seem to expand explosively and merge together to produce an area of almost solid black, which are the indicators of the onset of chaos. Numerical results obtained from the proposed switched SC-CNN Lorenz-like system are shown in Figure 1 with chaotic attractor projection, time domain response, bifurcation diagram, and Lyapunov exponents.

The Lyapunov exponents with given initial conditions are 0.059886, –0.032793, and -1.2566, as shown in Figure 1. The Lyapunov exponents of the switched SC-CNN system are calculated with 10^6 iterations using a fourth-order Runge–Kutta algorithm with a step size of $\Delta t = 0.01$.

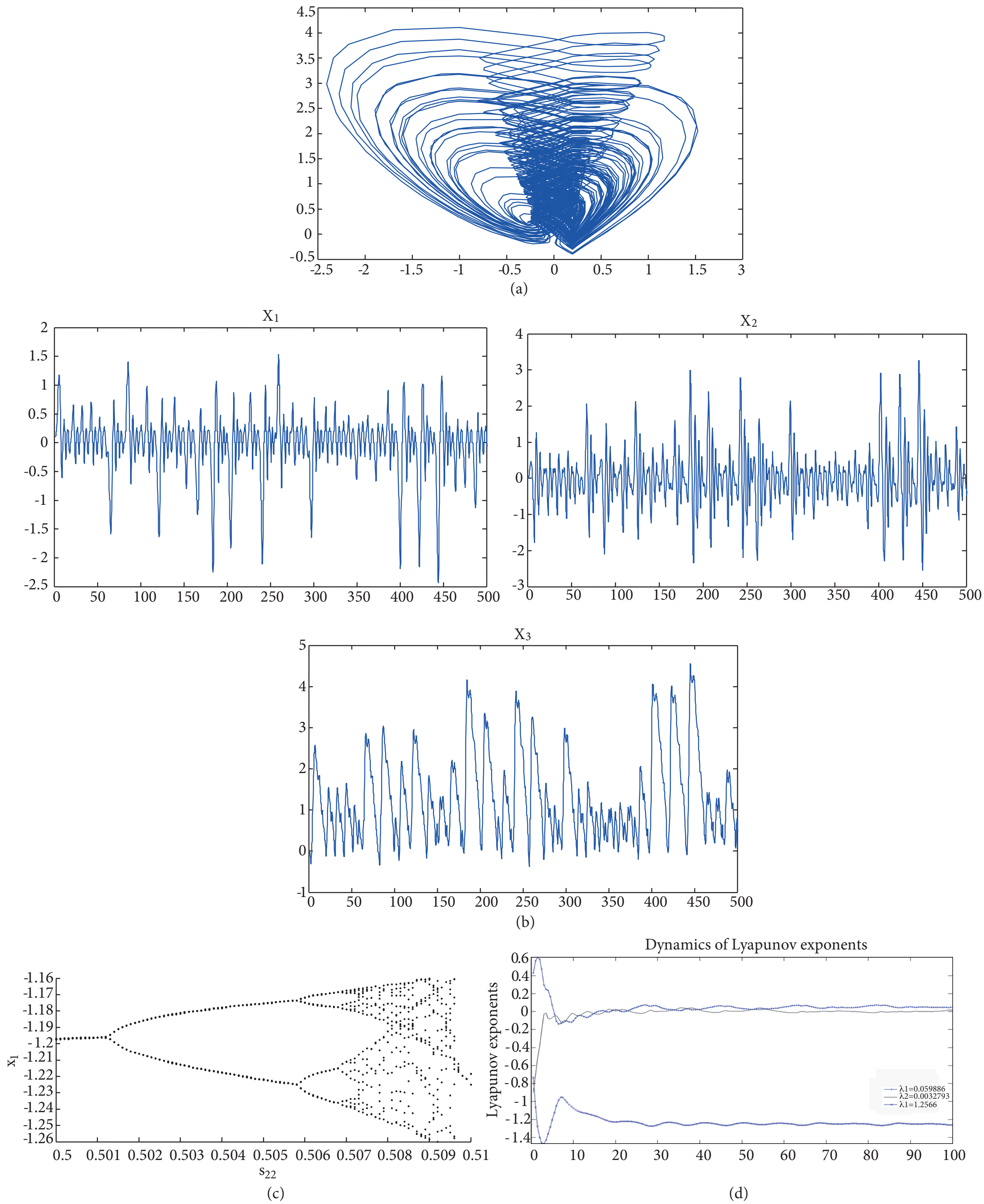

Figure 1. Numerical results of the switched-SC-CNN–based Lorenz-like system: (a) Chaotic attractor projection in (x_1–x_3) plane, (b) time response of x_1, x_2, and x_3, c) bifurcation diagram x_1 versus s_{22}, (d) Lyapunov exponents.

4. Experimental realization of the proposed switched SC-CNN system on field programmable analogue array (FPAA)

In recent days, more efficient and economical platforms have become a necessity in analogue dynamic system circuit design. FPAA, which is a reconfigurable and reprogrammable circuit platform, comes forward in the implementation of rich variety of systems by using analogue functions. A FPAA development board, AN231K04-QUAD4 type FPAA QuadApex produced by Anadigm (Oak Park, CA, USA), was used in the experimental work. In Figure 2, FPAA implementation scheme of the proposed system, the chaotic attractor projection in the $(x_1{-}x_3)$ plane and time responses of x_1 and x_3 are presented, respectively.

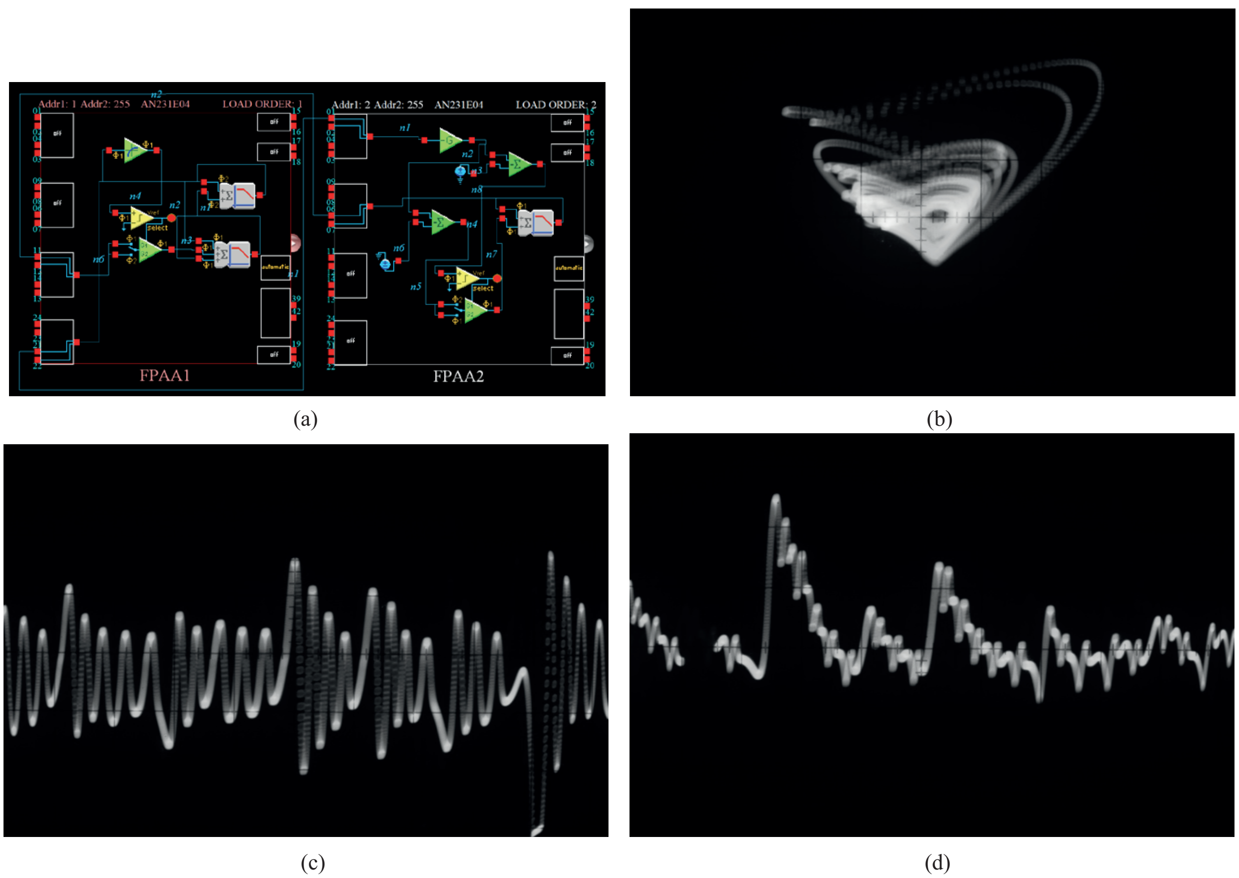

Figure 2. Experimental results of FPAA implementation of the switched-SC-CNN-based Lorenz-like system: (a) FPAA implementation scheme, (b) chaotic attractor projection in $(x_1 - x_3)$ plane, (c) time response of x_1, (d) time response of x_3.

The proposed system is built using two FPAA platforms. SUMFILTER blocks, consisting of integrators with up to three inputs and a single-pole low-pass filter, adjust the gains of the proposed circuit and generate the state variables of the proposed system via Laplace transforms. While the PWL output function of SC-CNN system is implemented with a user-defined TRANSFER FUNCTION block, the gains of the proposed system are obtained from the GAINHALF BLOCK. By using two sequential blocks, $n_{23} = \mathrm{sgn}(y_1)$ and $n_{31} = \mathrm{sgn}(x_1 - -i_3)$, functions can be generated in the GAINSWITCH BLOCK. In the GAINSWITCH BLOCK of FPAA1, a comparator is used to produce a reference value of ± 1 by comparing the output of the TRANSFER FUNCTION block with the ground. Then this value is switched to the SUMFILTER block to obtain $n_{23} =$

sgn(y_1). The expression $n_{31} = \mathrm{sgn}(x_1 - -i_3)$ is implemented in the FPAA2 platform with a comparator, which is used to produce a reference value of ± 1 by comparing the output of SUMINVERTER BLOCK with the ground. Similarly, this value is switched to the SUMFILTER block to obtain $n_{31} = \mathrm{sgn}(x_1 - i_3)$. The SUMINVERTER BLOCK is used to perform addition on its inputs with an inverter. In addition, the threshold value i_3 is generated by the DC VOLTAGE SOURCE block in FPAA2. In Table 2, FPAA implementation blocks are summarized with their symbols and explanations.

Table 2. FPAA implementation block descriptions.

FPAA implementation blocks		
SUMFILTER BLOCK	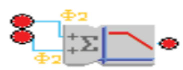	State equations x_1, x_2, and x_3 are obtained from SUMFILTER blocks. These blocks work as integrators using Laplace transfoms.
TRANSFER BLOCK		PWL output function of SC-CNN is implemented by a user-defined TRANSFER FUNCTION block. $\dot{y}_1, = {}^1/_2 \left(\lvert x_1 + 1\rvert - \lvert x_1 - 1\rvert\right)$
GAINHALF BLOCK		GAINHALF block, which is run in inverting mode, provides a gain that can be adjusted between 0.01 and 100.
SUMINVERTER BLOCK	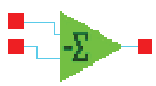	SUMINVERTER BLOCK performs addition with an inverter.
GAINSWITCH BLOCK	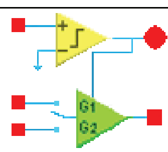	GAINSWITCH block, consisting of two sequential blocks, is used to obtain n_{23} = sgn(y_1) and n_{31} = sgn($x_1 - i_3$).
DC VOLTAGE SOURCE BLOCK	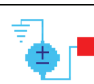	DC VOLTAGE SOURCE block is used for the i_3 threshold.

5. Conclusion

In this study, a switched-SC-CNN-based Lorenz-like system is introduced with numerical and experimental results. Some fundamental properties of the switched-SC-CNN-based Lorenz-like system, such as chaotic dynamics, chaotic attractors, bifurcation diagrams, eigenvalues, and Lyapunov exponents, have been investigated using the proposed system. The experimental results obtained from the FPAA comply with the numerical results. This study should not be considered only as an alternative investigation of Lorenz-like systems. It also demonstrates the Lorenz-like system's ability to imitate quadratic system dynamics without changing its original PWL output.

Acknowledgment

This work is supported by the Research Fund of Erciyes University (Project Code: FDK-2016-6757).

References

[1] Sparrow, C. The Lorenz Equations: Bifurcations, Chaos and Strange Attractors. 1st ed. New York, NY, USA: Springer-Verlag, 1982.

[2] Cuomo KM, Oppenheim AV, Strogatz SH. Synchronization of Lorenz-based chaotic circuits with applications to communications. IEEE T Circuits-II 1993; 40: 626-633.

[3] Chen G, Ueta T. Yet another chaotic attractor. Int J Bifurcat Chaos 1999; 9: 1465-1466.

[4] Liu C, Liu T, Liu L, Liu K. A new chaotic attractor. Chaos Soliton Fract 2004; 22: 1031-1038.

[5] Rikitake T. Oscillations of a system of disk dynamos. In: Mathematical Proceedings of the Cambridge Philosophical Society. Cambridge, UK: Cambridge University Press, 1958, pp. 89-105.

[6] Chua L, Yang L. Cellular neural networks: Theory. IEEE T Circuits-II 1988; 35: 732-745.

[7] Chua L. CNN: A paradigm for complexity. In: World Scientific Series on Nonlinear Science. Singapore: World Scientific Publishing, 1988, p. 31.

[8] Chua L, Roska T. The CNN paradigm. IEEE T Circuits-I 1993; 40; 147-156.

[9] Arena P, Baglio S, Fortuna L, Manganaro G. Chua's circuit can be generated by CNN cells. IEEE T Circuits-I 1995; 42; 123-125.

[10] Manganaro G, Arena P, Fortuna L. Cellular Neural Networks Chaos, Complexity and VLSI Processing. 1st ed. Berlin, Germany: Springer, 1999.

[11] Caponetto R, Lavorgna M, Occhipinti L. Cellular neural networks in secure transmission applications. In: CNNA'96; 24–26 June 1996; Seville, Spain. New York, NY, USA: IEEE. pp. 411-416.

[12] Günay E. MLC circuit in the frame of CNN. Int J Bifurcat Chaos 2010; 20: 3267-3274.

[13] Rössler OE. An equation for continuous chaos. Phy Lett A 1976; 57: 397-398.

[14] Arena P, Fortuna L, Rizzo A, Xibilia MG. Extending the CNN paradigm to approximate chaotic systems with multivariable nonlinearities. In: ISCAS 2000; 28–31 May 2000; Geneva, Switzerland. New York, NY, USA: IEEE. pp. 141-144.

[15] Lorenz EN. Deterministic nonperiodic flow. J Atmos Sci 1963; 20: 130-141.